Machining of bi-metallic aluminium-grey cast iron engine block - Process optimisation by means of FEM

Available online at www.sciencedirect.com

ScienceDirect

Procedia CIRP 117 (2023) 323–328

www.elsevier.com/locate/procedia

19th CIRP Conference on Modeling of Machining Operations

Machining of bi-metallic aluminium-grey cast iron engine block – process optimisation by means of FEM

Amir Malakizadi*, Lars Nyborg

Department of Industrial and Materials Science, Chalmers University of Technology, SE-412 96, Gothenburg, Sweden

* Corresponding author. Tel.: +46-31-772 63 77. *E-mail address:* amir.malakizadi@chalmers.se

Abstract

Bi-metallic design concept has been introduced in automotive industries to meet the increasingly tighter standards on carbon emission. Yet, machining of bi-metallic engine blocks is accompanied by several challenges like short tool life and long cycle times. This study presents a novel methodology that combines the concept of experimental design with Finite Element (FE) to optimise the tool performance and enhance the productivity when finish face milling of aluminium-grey cast iron engine blocks. This simulation-assisted approach led to an approximately 32% decrease in machining cycle time as compared to that of a reference cutting condition.

Keywords: FEM; Bi-metallic; Aluminium; Cast iron; Characterisation

1. Introduction

The increasingly tighter standards on fuel economy and emission rates have encouraged the automakers to introduce more advanced lightweight design concepts for engine components. The engine and its comprising parts have a high weight reduction potential, hence a robust design strategy for engine components can itself lead to a significant reduction in the overall weight of the cars and their fuel consumption [1]. The bi-metallic (compound) design concept is one of the well-established strategies for production of lightweight engines in the automotive industries. In this design concept, the aluminium structure of the engine block is combined with other materials to promote reinforcement, wear resistance and specific functions if necessary. For example, grey cast iron (GCI) liners and the main bearing caps made of sintered powder metallurgy (PM) steels are commonly integrated in the die-cast aluminium engine blocks [2] to enhance the engine performance whilst reducing its overall weight. Nevertheless, machining of components as such is often accompanied by several challenges; including limited tool life [3], poor surface finish and bond integrity between two materials [4] and long machining times. Due to remarkable differences in thermal and mechanical properties of the constituent materials, optimum machining of bi-metallic engine blocks demands special considerations. Wet condition is favourable for machining aluminium alloys to reduce built up edge (BUE) formation during cutting process, leading to improvement in the tool performance and the surface finish quality [5]. Dry condition is, on the other hand, recommended for intermittent machining of GCI parts to avoid thermal cracking and chipping the cutting edge [6]. Hence, an optimal strategy for machining of bi-metallic components – to meet the demands on the surface quality, machining time and tool life simultaneously – has remained a challenge in the automotive industries.

Several investigations have been performed on the machining of bi-metallic components. Denkena et al. [7] conducted a dedicated experimental study to identify the critical aspects of machining bi-metallic aluminium-spherical cast iron (SGI) compounds. The experimental results showed that the cutting forces and temperatures depended on the cutting direction, and the thermo-mechanical loads on the inserts were minimised when the tool first cut through the soft

10.1016/j.procir.2023.03.055

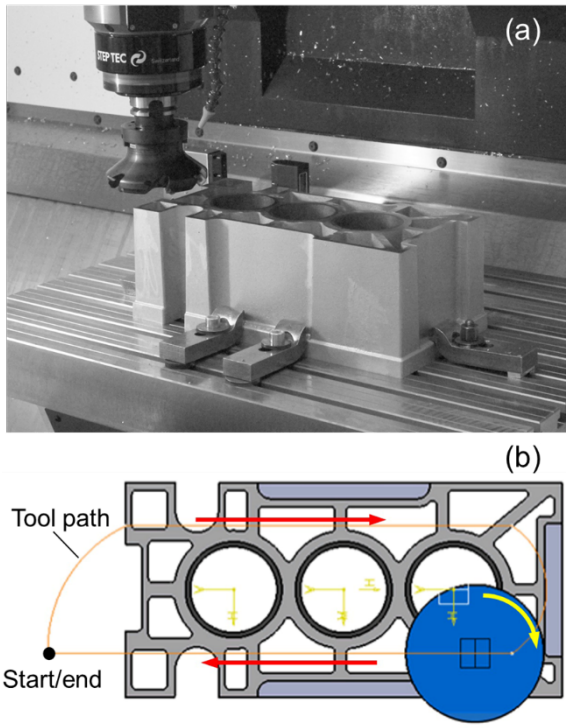

Fig. 1. (a) The experimental setup for tool life test (b) and top view of bi-metallic sample indicating the programmed tool path.

aluminium alloy. Hence, the tool performance when machining of bi-metallic components was strongly influenced by the cutting direction and the thermo-mechanical properties of the constituent materials. Even though such experimental approaches provide a complete picture of machining operation, it may be impractical to run costly experiments for every newly developed bi-metallic compounds. To this end, Malakizadi et al. [8] proposed the use of 3D FE simulations to estimate the thermo-mechanical loads induced on the cutting edges under operational conditions.

In this study, this methodology is further extended to determine the optimum cutting condition when machining bi-metallic aluminium-grey cast iron engine blocks. The focus was placed on finish face milling the top-deck surfaces, because of its utmost importance to accomplish the tight surface finish requirements necessary for a satisfactory sealing between cylinder head and the engine block. Here, Response Surface Methodology (RSM) is used to establish the relationship between the cutting parameters and the range of thermal stresses induced on the cutting edge under operational condition estimated using 3D FE simulation of milling process. The optimum cutting condition was then determined by evaluation of the range of thermo-mechanical loads and the effective number of thermal cycles per unit length of cut, to which the tool is exposed during machining operation. Finally, the credibility of the presented methodology was experimentally verified.

2. Experimental procedure

Tool life tests were performed on bi-metallic AlSi9Cu3Fe aluminium-GCI component-like samples. These workpieces were designed to mimic the details of top-deck surface of the engine blocks and were produced in similar manner in terms of material specification and casting procedure. The experimental set-up for the tool life tests is shown in Fig. 1a. The geometry of the bi-metallic workpiece and the programmed machining path for tool life tests are shown in Fig.1b.

Tool life tests were conducted at four different cutting conditions, shown in Table 1. The R245-125Q40-12L cutter with 125 mm effective diameter was equipped with two Sandvik R245-12T3E-KL H13A uncoated cemented carbide inserts and a CD10 PCD wiper to fulfil the demands on the quality of machined surfaces. The axial run-out of wiper was closely adjusted to lie within the range exploited in production line. The tool life criterion for uncoated carbides was set as either 0.3 mm average flank wear width (VB_B) or excessive chipping on the cutting edge. The cutting tools were examined regularly (every 5 machining passes) to monitor the wear evolution. All machining tests were carried out under wet condition to meet surface finish requirements. Emulsion with 7% concentration (CareCut 600 E) was used as the coolant.

Table 1. The cutting conditions used for tool life tests.

Cutting condition	v_C (m/min)	f_Z (mm)	a_p (mm)
A	150	0.15	0.50
B	150	0.25	0.50
C	250	0.15	0.50
D	250	0.25	0.50

3. Modelling procedure

3.1. FE simulation of cutting process

Face milling operation was modelled using DEFORM 3D commercial code. The tool and a segment of the workpiece in the vicinity of the cutting edge were generated using CATIA modelling software. In this step, the tool and workpiece were also positioned based on the cutting conditions and tool angles. The tool was assumed as a rigid body; however, the heat transfer was allowed within the tool during cutting simulation. Only 8 degrees of cut was simulated to reduce the computational time and the uncut chip thickness assumed constant at its maximum through the cut, to simulate the maximum thermo-mechanical load on the cutting-edge during tool engagement. The element size in the vicinity of the cutting edge was controlled during the simulation by means of mesh window technology, with 0.01 mm and 0.02 mm minimum element size for tool and workpiece, leading to approximately 90000 and 120000 elements for the tool and work material, respectively. The viscoplastic behaviour of the workpiece material was simulated using Johnson-Cook (JC) constitutive model:

$$\sigma = (A + B\varepsilon^n)\left(1 + C\,ln\left(\frac{\dot{\varepsilon}}{\dot{\varepsilon}_0}\right)\right)\left(1 - \left(\frac{T - T_r}{T_m - T_r}\right)^m\right) \quad (1)$$

where ε is the strain, T is the temperature and $\dot{\varepsilon}$ is the strain rate. A, B, C, n and m represent the material parameters, $\dot{\varepsilon}_0$ is the reference strain rate and T_m and T_r are melting and initial temperatures of the workpiece material, respectively. Table 2 shows the JC material parameters for GCI and AlSi9Cu3Fe, determined using an inverse modelling of orthogonal cutting process [8, 9]. A large heat transfer coefficient is assumed at

the tool-chip interface (h = 10^5 kW/m^2°C). In addition, a heat transfer coefficient of 2500 W/m^2°C was applied on the free surface to account for coolant effects. Experimental temperature measurements for a number of tool-work material combinations, including aluminium alloys [10], clarifies the viability of assumed thermal boundary condition. The sticking-sliding frictional stress distribution at the tool-chip interface was approximated using a pressure dependent shear friction model:

$$\tau_f = [1 - exp(-\alpha P)]k \quad (2)$$

where τ_f is the shear stress, k is the shear strength of work material and P is the normal stress at tool-chip interface. α represents the model parameters. As evident, at high contact pressures close to the cutting edge, the shear stress equals to shear strength of the work material (sticking region), and it gradually decreases as the contact pressure drops. Eq. (2) was implemented using a Fortran subroutine. Table 3 shows the optimum sets of parameters for each tool-work material combination. The thermal properties of the aluminium alloy and GCI were obtained from JMatPro^{TM} material modelling software [11] and Data Handbook for Grey Irons [12], while the thermal properties of the tool material are taken from [9].

Table 2. JC material parameters for GCI and AlSi9Cu3Fe [8].

Mat.	*A* (MPa)	*B* (MPa)	*C* (-)	*n* (-)	*m* (-)	*α* (-)	$\dot{\varepsilon_0}$ (s^{-1})	T_m (°C)
Al	250	157	0.024	0.158	0.9	0.012	1	495
GCI	470	250	0.004	0.1	1.1	0.0035	1	1200

3.2. FE simulation of thermo-mechanical stresses

The induced thermo-mechanical stresses on the cutting edge were predicted using a decoupled stress analysis approach (DEFORM, 2012) combined with the concept of experimental design and Response Surface Methodology (RSM). Here, the cutting operation was initially simulated for different sets of cutting parameters including the cutting speed (v_c), feed per tooth (f_z) and depth of cut (a_p) – varying between 150-250 m/min, 0.15-0.25 mm and 0.35-0.50 mm, respectively. The Central Composite Design (CCD) algorithm implemented in MATLAB® was used to generate 15 different sets of input parameters within the range of cutting conditions mentioned above. After completion of the cutting simulations, the calculated nodal forces were interpolated on the tool surfaces. The tool was converted to an elastic object and the appropriate structural constraints were imposed on the model far from the cutting edge to avoid rigid-body motion. Also, the heat transfer simulation was excluded in this step to ensure that the induced stresses on the cutting edge were solely due to mechanical loads. In order to calculate the thermally induced stresses, the simulation environment was reset by removing nodal forces and displacements on the tool. The nodal temperature at the end of cutting simulations were instead interpolated on the meshed tool and the thermal and structural boundary conditions were assigned on the corresponding surfaces. The relationship between the induced thermal stress and the cutting parameters was then expressed as a second order polynomial using regression analysis.

4. Results and discussion

4.1. Tool life results and wear mechanisms

A detailed analysis of the worn tools using scanning electron microscope (SEM) revealed thermal cracking as the dominant wear mechanism for uncoated cemented carbides at all cutting conditions given in Table 1. These cracks can potentially cause flaking and fracture of a portion of the tool edge in later stages as the operation proceeds. Flank wear progression was also noted on the cutting edges; however, the extent of wear during machining tests was smaller than the pre-set flank wear criterion (see Section 2) and the tool performance was limited by thermal cracking and chipping of the cutting edges, as shown in Fig. 2.

Similar wear mechanism was observed during face milling the aluminium-GCI engine blocks under operational conditions using CBN inserts [8]. Bhatia et al. [13, 14] classified the types of cracks that generated on cemented carbide tools during intermittent cutting on the basis of the dominant cause of tool failure. It was shown that the types of cracks varied with the cutting conditions. The cracks due to mechanical loads were developed on the rake face and almost parallel to the cutting edge and solely seen when operating at low speeds and high feed rates. This type of cracks was also referred to as mechanical fatigue cracks [15]. The comb cracks, on the other hand, initiated and developed due to cyclic thermal expansion and contraction of surface layers on the tool edge during intermittent cutting, and they were invariably seen at high cutting speeds and low feed rates [13]. These cracks, also referred to as thermal cracks, formed perpendicular to the cutting edge and brought about the final fracture of the tool edge as the machining operation proceeded. At high cutting speeds and moderate feed rates, the cutting edge was subjected to moderately high thermo-mechanical loads, which promoted the formation of both mechanical and thermal cracks on the cutting edge [13].

Thermal cracking has been commonly reported for various types of tools during milling GCI parts. Da Silva et al. [6] observed thermal cracking, in addition to abrasion and adhesion wear, on Al_2O_3 coated carbides when face milling of pearlitic grey cast irons at high cutting speeds, even under dry

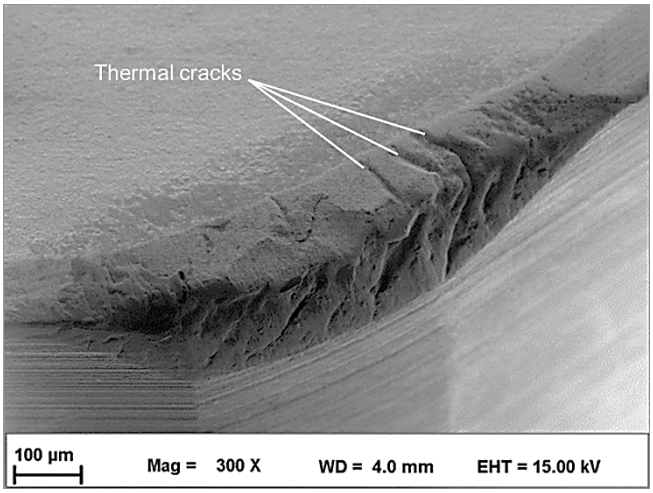

Fig.2. Thermal cracks developed on the cutting edge at cutting condition C, see Table 1.

condition. Dias and Diniz [16] reported similar behaviour when face milling fully pearlitic and ferritic-pearlitic grey cast iron components using ceramic and multi-layered CVD coated inserts. Edge rounding and steady flank wear progression were, on the other hand, reported as the dominant wear modes for carbide tools when machining aluminium alloys. Relatively, small temperature variations during intermittent machining aluminium alloys ruled out the likelihood of initiation of thermal fatigue cracks; hence, abrasion and/or adhesion are envisaged to be the main wear mechanisms. König et al. [17] reported that the flank wear was the main tool wear mode for uncoated cemented carbides when machining Al-Si alloys, and the wear rate depended strongly on the silicon content and the casting procedure due to the associated influences of distribution and morphologies of the silicon particles. Similarly, Ng et al. [5] observed edge rounding as the dominant wear mode when face milling of Al-Si alloys. These observations suggested that large temperature variations on the tool edge when cutting through the GCI liners plays a key role, limiting tool performance.

Fig. 3 shows the number of machining passes prior to tool failure as well as the cycle time for different cutting conditions, given in Table 1. The cycle time (i.e., the time takes for a single machining pass) was calculated in seconds as:

$$t_C = 60\frac{l_m}{v_f} \tag{3}$$

where l_m is the machining length in mm (i.e., tool path in Fig. 1b), and v_f is the table feed in mm/min which can be given as:

$$v_f = \Omega Z_C f_z \tag{4}$$

In Eq. 4, Ω is the spindle speed in RPM and Z_C and f_z represent the effective number of inserts (here Z_C = 3) and feed per tooth in mm, respectively. As evident, the cutting conditions B and C resulted in similar cycle times, whilst the cutting condition B outperformed the cutting condition C in term of tool life.

4.2. FE simulation results and induced thermal stresses

Preliminary FE simulation results under the cutting condition C showed that the maximum temperature on the cutting edge is nearly two times larger when machining of GCI as compared to that of aluminium machining. This is consistent with the temperature measurement results reported by Stephenson and Ali [18] and Denkena et al. [7] for various grades of cast iron and aluminium alloys. Hence, the observed thermal cracks were mainly due to larger temperature fluctuations when cutting through the grey cast iron liners – in agreement with the experimental observation presented by Da Silva et al. [6] and Dias and Diniz [16]. The focus was therefore placed solely on simulation of machining operation for the grey cast iron.

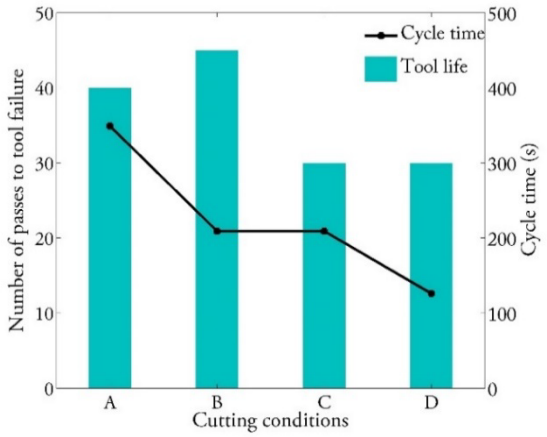

Fig. 3. The number of passes to tool failure and calculated cycle times for various cutting conditions given in Table 1.

The distribution of induced thermal (von Mises) stresses on the cutting edges when machining GCI at different cutting conditions is also shown in Fig. 4 (see Table 1). Fig. 5 shows the variation of the maximum thermal stress on the tool edge as a function of cutting parameters for an arbitrary cutting condition created using the calibrated quadratic model. It should be noted here that the determined response surface can only be used to predict the maximum thermal stress on the cutting edge within the incorporated domain of experimental design.

4.3. Determination of optimum cutting condition

The tool life test results presented in Fig. 3 shows that the maximum tool life was attained at cutting condition B, while the FE simulation results suggested that lowest maximum thermal stress ($\sigma_{th,max}$) is resulted when machining under the cutting condition A (see Fig. 4). This discrepancy between tool life tests and simulation results can be explained by taking into account the influence of number of thermal cycles during interrupted cutting processes such as milling operation. As stated by Yellowley and Barrow [19] and Bhatia et al. [13, 14], under the conditions in which thermal fatigue cracking is dominant, the range of thermal stresses on the cutting edge and the number of thermal cycles influence the tool performance and therefore both need to be taken into account for tool life optimisation. The number of tool engagements per unit length of cut (N_C) when milling an ideal solid block (without any cavity) can simply be calculated as:

$$N_C = \frac{1000}{Z_C f_z} \tag{5}$$

where Z_C is the number of inserts and f_z is the feed per tooth in mm. The effective number of tool engagements (N_E) with the GCI liner embedded in the bi-metallic workpieces is proportional to N_C. Even though the maximum uncut chip thickness constantly varies during machining due to the cylindrical geometry of the liners, N_E depends solely on the number of inserts and the feed per tooth as the tool path remains unchanged (as shown in Fig. 1). This parameter can thus be used as a relative factor to explain the experimental tool life measurements shown in Fig. 3. For example, in case of condition A, N_E is about 67% larger than that of cutting condition B, while the thermal stress on the cutting edge is 24% smaller than that of cutting condition B. Thus, the larger number of tool engagements under the condition A led to only slightly lower tool life compared to that of cutting condition B (see Fig. 3), despite lower thermally induced stresses under this cutting condition.

Fig. 6 shows the state of cutting tool geometry after 10 passes under cutting conditions B and C. The cycle times were similar for both cutting conditions (see Fig. 3); however, the N_E was 67% larger for cutting condition C compared to that of cutting condition B. As evident, the thermal cracks were only generated on the tool edge at cutting condition C, although the FE simulation results presented in Fig. 4 indicate nearly similar range of maximum thermal stress on the tool. It should also be noted here that when machining at larger feed per tooth, FE simulations suggested that the location of maximum thermally induced stress is further away from the cutting edge, compare the corresponding cutting conditions in Fig. 4. These two examples prove that N_E and $\sigma_{th,max}$ can be used to determine optimum tool life when machining of bi-metallic workpieces.

Two different scenarios can be considered for tool life optimisation: (1) the cutting condition under which the maximum tool life is achieved, and (2) the cutting condition that results in the shortest cycle time while meeting a certain target on tool life. Here, these two optimisation scenarios were referred to as OPT1 and OPT2, respectively. The optimum condition in terms of tool life (OPT1) can be achieved when the feed per tooth is maximised while the thermal stress induced on the cutting edge is minimised. On the other hand, the cutting condition under which the shortest machining time is resulted (OPT2) can be determined by maximising the feed per tooth while the range of induced thermal stress on the cutting edge is held equal to that of a reference cutting condition. Here we consider cutting condition B as the reference cutting condition, giving the best tool performance during tool life tests (see Fig. 3). However, increasing feed per tooth also increases the range of alternating mechanical stresses on the cutting edge as well as the volume of the tool material experiences high mechanical loads. Both these factors shown to play significant roles in the fatigue properties of cemented carbides [20]. Hence, increasing feed per tooth can shift the predominant tool failure mechanism from thermal fatigue cracking to mechanically induced cracking and sudden fracture of the cutting edge (premature tool failure), as also shown by Bhatia et al. [13]. However, reducing a_p from 0.5 to 0.35 mm can, to some extent, alleviate the severity of mechanical loads applied on the cutting edge due to an increase in f_z from 0.15 to 0.25 mm. In addition, FE simulation results suggest that $\sigma_{th,max}$ reduces with a decrease in a_p, as shown in Fig. 5. These two observations enable the optimisation of the cycle time as compared to that of the reference cutting condition B.

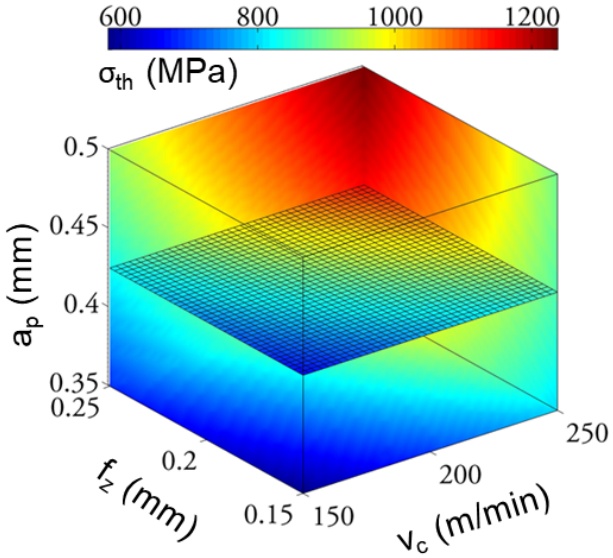

Fig. 5. The maximum thermally-induced stress on the tool edge ($\sigma_{th,max}$) when machining of GCI as a function of cutting parameters.

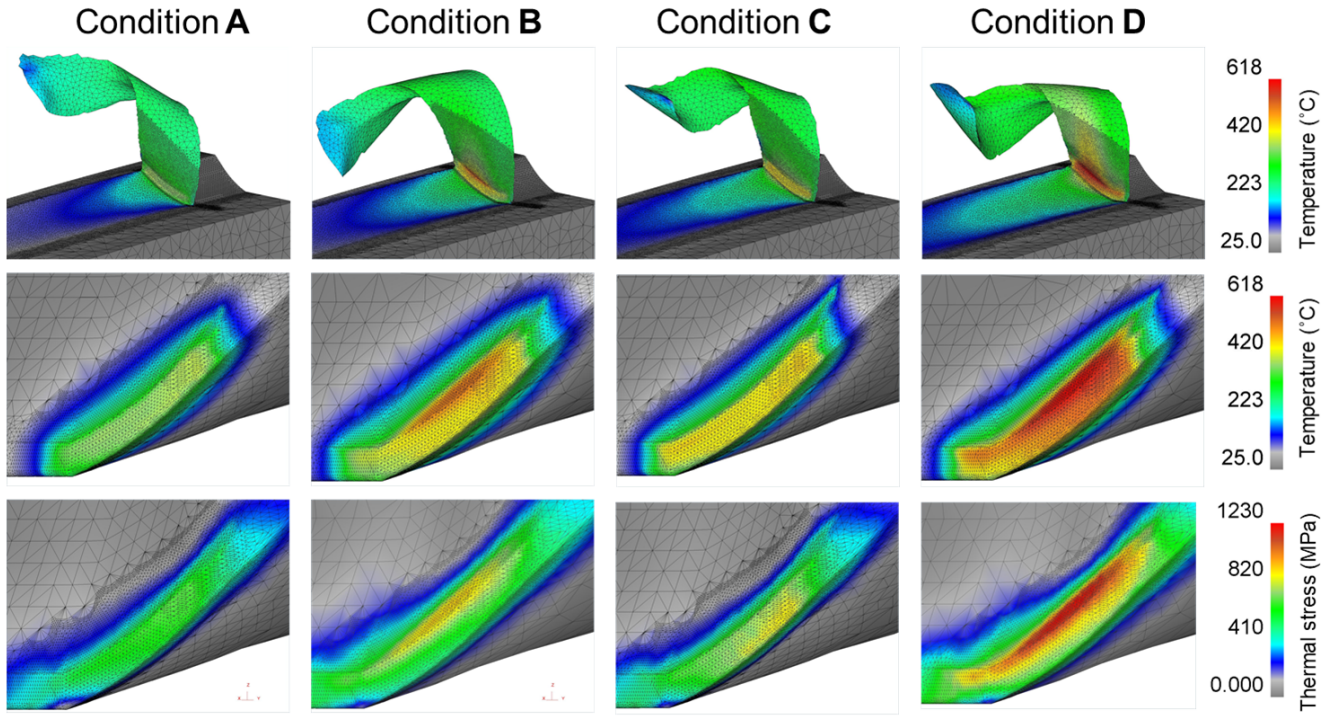

Fig. 4. Chip formation, maximum temperature distribution and maximum thermal induced due to temperature fluctuation (maximum temperature to room temperature) when machining of GCI under cutting conditions A-D given in Table 1.

This can be done by adjusting the cutting speed to such a level that the thermal stress on the cutting-edge stays nearly the same level as that of the reference cutting condition B. To achieve this, the smallest range of a_p should be selected. Moreover, to achieve the smallest possible N_E, the highest feed per tooth within the range design of experiment should be selected (f_z = 0.25 mm).

Table 3 shows the comparison between the optimum conditions OPT1 and OPT2 determined using the described strategies and the reference cutting condition B. Experimental tool life tests were also performed under conditions OPT1 and OPT2 following the same tool path shown in Fig.1b to assess the potential of the hybrid optimisation approach presented in this study. As evident, the cutting condition OPT2 yields nearly the same tool life, while the cycle time was reduced by 32% for a similar tool path shown in Fig. 1. Cutting condition OPT1, on the other hand, led to 56% increase in tool life compared to the reference condition B.

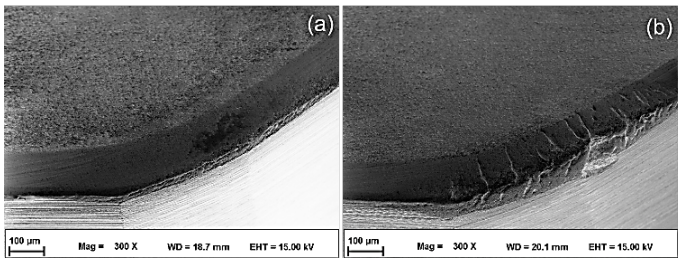

Fig. 6. The worn tool geometry after 10 machining passes at cutting condition (a) B and (b) C shown in Table 1.

Table 3. The optimum cutting condition in terms of tool life and cycle time.

Cond.	v_C *(m/min)*	f_Z *(mm)*	a_p *(mm)*	$\sigma_{th,max}$ *(MPa)*	life *(No.)*	t_C *(s)*
Cond. B	150	0.25	0.50	911	45	220.2
OPT 1	150	0.25	0.35	676	70	220.2
OPT 2	220	0.25	0.35	926	40	150.2

5. Conclusion

This study presented a methodology based on the concept of experimental design and Response Surface Methodology (RSM) for tool life optimisation when finish face milling of bi-metallic aluminium-grey cast iron engine blocks. It was shown that the range of thermal stresses and the number of thermo-mechanical cycles are both needed to be taken into account during process optimisation. The methodology presented in this study led to 32% saving in machining times during finishing operations compared to a reference condition, without the need to perform extensive experimental tool life tests. This approach can be extended for tool life optimisation during intermittent machining operations such as milling under the conditions in which thermal cracking is the predominant tool failure mechanism.

Acknowledgements

Financial support by the Swedish Agency for Innovation Systems (VINNOVA) and the Area of Advance Production at Chalmers University of Technology are gratefully acknowledged. Supports from Dr. M. Ibrahim Sadik and Mr. Lars Hellström from Sandvik Coromant are acknowledged.

References

[1] R. Marquard, W. Schoffmann, and F. Beste, Lightweight Design-A Challenge for Modern Passenger Car Engines, JSAE Annual Congress, Japan, 2001.
[2] D. C. Corrêa, W. F. Sales, S. C. Santos, and E. S. Palma, Machinability of bimetallic bearings using cemented carbide tools: evaluation of the wear mechanisms, Journal of Materials Processing Technology, vol. 159, no. 3, pp. 435-444, 2005.
[3] B. Denkena, D. Boehnke, and P. Dziewiecki, Tool behavior at alternating thermo-mechanical loads during milling of compounds out of aluminum and spheroidal cast iron, Production Engineering, vol. 2, no. 4, pp. 351-356, 2008.
[4] M. Uthayakumar, G. Prabhaharan, S. Aravindan, and J. V. Sivaprasad, Machining studies on bimetallic pistons with cbn tool using the Taguchi method–Technical Communication, Machining Science and Technology, vol. 12, no. 2, pp. 249-255, 2008.
[5] E. G. Ng, D. Szablewski, M. Dumitrescu, M. A. Elbestawi, and J. H. Sokolowski, High speed face milling of a aluminium silicon alloy casting, CIRP Annals - Manufacturing Technology, vol. 53, no. 1, pp. 69-72, 2004.
[6] M. B. Da Silva, V. T. G. Naves, J. D. B. De Melo, C. L. F. De Andrade, and W. L. Guesser, "Analysis of wear of cemented carbide cutting tools during milling operation of gray iron and compacted graphite iron," Wear, vol. 271, no. 9–10, pp. 2426-2432, 2011.
[7] B. Denkena, L. De Leon, A. Lucas, and R. Meyer, Thermomechanical tool load in the machining of spheroidal cast iron–aluminium compounds, International Journal of Machining and Machinability of Materials, vol. 10, pp. 1-17, 2011.
[8] A. Malakizadi, I. Sadik, and L. Nyborg, Wear Mechanism of CBN Inserts During Machining of Bimetal Aluminum-grey Cast Iron Engine Block, Procedia CIRP, vol. 8, no. 0, pp. 188-193, 2013.
[9] A. Malakizadi, S. Cedergren, I. Sadik, and L. Nyborg, Inverse identification of flow stress in metal cutting process using Response Surface Methodology, Simulation Modelling Practice and Theory, vol. 60, pp. 40-53, 2016.
[10] G. Rotella, O. W. Dillon Jr, D. Umbrello, L. Settineri, and I. S. Jawahir, Finite element modeling of microstructural changes in turning of AA7075-T651 Alloy, Journal of Manufacturing Processes, vol. 15, no. 1, pp. 87-95, 2013.
[11] Z. Guo, N. Saunders, J. P. Schillé, and A. P. Miodownik, Material properties for process simulation, Materials Science and Engineering: A, vol. 499, no. 1–2, pp. 7-13, 2009.
[12] Data Handbook for Grey Irons. Castings Development Centre, 1997.
[13] S. M. Bhatia, P. C. Pandey, and H. S. Shan, Failure of cemented carbide tools in intermittent cutting," Precision Engineering, vol. 1, no. 3, pp. 148-152, 1979.
[14] S. M. Bhatia, P. C. Pandey, and H. S. Shan, "Failure of cemented carbide tools when executing intermittent cuts " Journal of Manufacturing Science and Engineering vol. 101, no. 4 pp. 391-396, 1979.
[15] A. C. A. Melo, J. C. G. Milan, M. B. Silva, and Á. R. Machado, Some observations on wear and damages in cemented carbide tools, Journal of the Brazilian Society of Mechanical Sciences and Engineering, vol. 28, pp. 269-277, 2006.
[16] L. R. M. Dias and A. E. Diniz, Effect of the gray cast iron microstructure on milling tool life and cutting force, Journal of the Brazilian Society of Mechanical Sciences and Engineering, vol. 35, no. 1, pp. 17-29, 2013.
[17] W. König and D. Erinski, Machining and machinability of aluminium cast alloys, CIRP Annals - Manufacturing Technology, vol. 32, no. 2, pp. 535-540, 1983.
[18] D. A. Stephenson and A. Ali, Tool Temperatures in Interrupted Metal Cutting, Journal of Engineering for Industry, vol. 114, no. 2, pp. 127-136, 1992.
[19] I. Yellowley and G. Barrow, The influence of thermal cycling on tool life in peripheral milling, International Journal of Machine Tool Design and Research, vol. 16, no. 1, pp. 1-12, 1976.
[20] H. Chandrasekaran, Fracture of Carbide Tools in Intermittent Cutting, in Science of Hard Materials, R. K. Viswanadham, D. J. Rowcliffe, and J. Gurland Eds.: Springer US, 1983, ch. 40, pp. 735-755.